Additive Noise Induces Front Propagation

M. G. Clerc, C. Falcon, and E. Tirapegui
Departamento de Física, Facultad de Ciencias Físicas y Matemáticas, Universidad de Chile, Casilla 487-3, Santiago, Chile
(Received 16 August 2004; published 14 April 2005)

The effect of additive noise on a static front that connects a stable homogeneous state with an also stable but spatially periodic state is studied. Numerical simulations show that noise induces front propagation. The conversion of random fluctuations into direct motion of the front's core is responsible of the propagation; noise prefers to create or remove a bump, because the necessary perturbations to nucleate or destroy a bump are different. From a prototype model with noise, we deduce an adequate equation for the front's core. An analytical expression for the front velocity is deduced, which is in good agreement with numerical simulations.

DOI: 10.1103/PhysRevLett.94.148302 PACS numbers: 82.40.Ck, 05.40.Ca

The description of macroscopic matter, i.e., matter composed of a large number of microscopic constituents, is usually done using a small number of coarse-grained or macroscopic variables. When spatial inhomogeneities are considered these variables are spatiotemporal fields whose evolution is determined by deterministic partial differential equations (PDE). This reduction is possible due to a separation of time scales, which allows a description in terms of the slowly varying macroscopic variables, which are in fact fluctuating variables due to the elimination of a large number of fast variables whose effect can be modeled including suitable stochastic terms (noise) in the PDE. The influence of noise in nonlinear systems has been the subject of intense experimental and theoretical investigations [1–6]. Far from being merely a perturbation to the idealized deterministic evolution or an undesirable source of randomness and disorganization, noise can induce specific and even counterintuitive dynamical behavior. The most well-known examples in zero dimensional systems are noise-induced transition [1] and stochastic resonance [2]. More recently, examples in a spatial extended system are noise-induced phase transition [3], noise-induced patterns [4], stochastic spatiotemporal intermittency [5], and noise-induced traveling waves [6]. Here, we will focus on the effect of additive noise in front propagation. The concept of front propagation emerged in the field of populations dynamics [7], and the interest in these types of problems has been growing steadily in chemistry, physics, and mathematics. In physics, front propagation plays a central role in a large variety of situations, ranging from reaction diffusion models to general pattern forming systems (see the review in [8] and references therein). The influence of multiplicative noise in a globally stable state invading an unstable or metastable state, a *front solution*, has been extensively studied, particularly concerning the issue of velocity selection [9].

The aim of this Letter is to study the effect of noise in a motionless front that connects a stable homogeneous state with an also stable but spatially periodic state. Numerical simulation of this type of front shows that noise induces front propagation, that is, one state invades the other one. From a prototype model that exhibits this type of front, the subcritical Swift-Hohenberg equation with additive noise, we deduce an equation for the front's core, which is characterized by a periodic asymmetrical potential plus additive noise. The conversion of random fluctuations into directed motion of the front's core is responsible for front propagation. We obtain an analytical expression for the velocity of the front, which is proportional to Kramer's rate, in the weak noise intensity limit. This expression is in good agreement with numerical simulations.

A front that connects two stable homogeneous states in a variational system with a known free energy, permanently propagates from the state with higher free energy to the state with lowest free energy [8]. However, the front is static when both states are energetically equal, i.e., in the *Maxwell point*. This picture changes in the case of a front

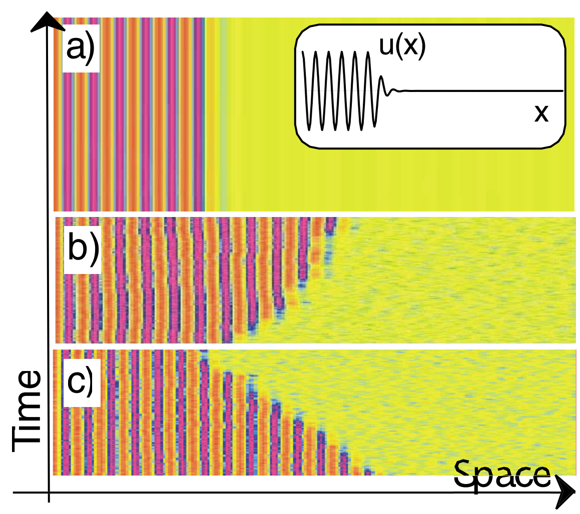

FIG. 1 (color online). Spatiotemporal evolution of Eq. (1), with time running up. The gray scale is proportional to field u. The inset figure is the initial condition. The parameters have been chosen $\varepsilon = -0.16$, $\nu = 1.0$, $q = 0.7$. (a) $\eta = 0.0$, (b) $\eta = 0.4$, and (c) $\varepsilon = -0.175$, $\eta = 0.5$.

that connects a stable homogeneous state with an also stable but spatially periodic one. This front exhibits a *locking phenomena* in a region of parameters known as the pinning range [10], in which the front does not move. When additive white noise is taking into account, one may expect random fluctuations of the interface between the two states (front's core). However, numerical simulations in a one dimensional extended system show that the front propagates from one state to the other with a stochastic velocity, as is illustrated in Fig. 1. The numerical method used in the simulation is the Runge-Kutta algorithm with time step equal 0.01, and spatial mesh 1/400. Depending on the region of parameters, the front can propagate to the periodic spatial state or to the homogeneous one.

In order to understand the mechanism through which noise induces propagation, we consider a prototype model that exhibits this type of front (subcritical Swift-Hohenberg equation with noise [8])

$$\partial_t u = \varepsilon u + \nu u^3 - u^5 - (\partial_{xx} + q^2)^2 u + \sqrt{\eta}\zeta(x, t), \quad (1)$$

where $u(x, t)$ is an order parameter, $\varepsilon - q^4$ is the bifurcation parameter, q is the wave number of periodic spatial solutions, ν the control parameter of the type of bifurcation (supercritical or subcritical), $\zeta(x, t)$ is a Gaussian white noise with zero mean value and correlation $\langle\zeta(x, t)\zeta(x', t')\rangle = \delta(x - x')\delta(t - t')$, and η represents the intensity of the noise. The model (1) describes the confluence of a stationary and an spatial subcritical bifurcation, when the parameters scale as $u \sim \varepsilon^{1/4}$, $\nu \sim \varepsilon^{1/2}$, $q \sim \varepsilon^{1/4}$, $\partial_t \sim \varepsilon$, and $\partial_x \sim \varepsilon^{1/4}$ ($\varepsilon \ll 1$). This bifurcation is of codimension three. The above model is often employed in the description of patterns observed in Rayleigh-Bénard convection [8].

For small and negative ν and $9\nu^2/40 < \varepsilon < 0$, the system exhibits coexistence between a stable homogenous state $u = 0$ and a periodic spatial one $u = \sqrt{\nu}(\sqrt{2(1 + \sqrt{1 + 40\varepsilon/9\nu})}\cos(qx)) + o(\nu^{5/2})$. In this parameter region, one finds a front between these two states. A front between a homogeneous and a spatial oscillatory state can be described by the ansatz

$$u = \sqrt{\frac{2\nu}{10}}\varepsilon^{1/4}\Big\{A\Big(y = \frac{3\sqrt{|\varepsilon|}}{2\sqrt{10q}}x,\\ \tau = \frac{9\nu^2|\varepsilon|}{10}t\Big)e^{iqx} + w_1(x, y, \tau)\Big\} + \text{c.c.}, \quad (2)$$

where $A(y, \tau)$ is the envelope that describes the front solution, $w_1(x, y, \tau)$ is a small correction function of order ε, and $\{y, \tau\}$ are slow variables. In this ansatz, we consider q is order one or larger than the other parameters. Introducing the above ansatz in Eq. (1) and linearizing in w_1, we find the following solvability condition

$$\partial_\tau A = \epsilon A + |A|^2 A - |A|^4 A + \partial_{yy} A \\ + \Big(\frac{A^3}{9\nu} - \frac{A^3|A|^2}{2}\Big)e^{2iqy/(a\sqrt{|\varepsilon|})} - \frac{A^5}{10}e^{2iqy/(a\sqrt{|\varepsilon|})} \\ + \frac{\sqrt{\eta}b}{|\varepsilon|^2}e^{2iqy/(a\sqrt{|\varepsilon|})}\zeta(y, \tau), \quad (3)$$

where $\epsilon \equiv 10\varepsilon/9\nu^2$, $a \equiv 3\nu/2\sqrt{10}q$, and $b \equiv 10^{9/4}/81\nu^4$. The deterministic terms proportional to the exponential are nonresonant, that is, one can eliminate these terms by an asymptotic change of variable. Furthermore, they have rapidly varying oscillations in the limit $\epsilon \to 0$. Hence, one usually neglects these terms. When one considers only the deterministic resonant terms, the first line of (3), it is straightforward to show that the system exhibits a front solution between two homogeneous states, 0 and $\sqrt{(1 + \sqrt{1 + 4\epsilon})/2}$, when $\epsilon < 0$. This front propagates from the stable state (lowest free energy) to the metastable one, and it is static when the Maxwell point is reached $\epsilon_M = -3/16$, and it has the form

$$A_\pm(y) = \sqrt{\frac{3/4}{1 + e^{\pm\sqrt{3/4}(y - y_0)}}}e^{i\theta},$$

where y_0 is the position of the front's core, and θ is an arbitrary phase. In the neighborhood of ϵ_M the front propagates by a velocity given approximately by $\Delta = 3d/8(\epsilon - \epsilon_M)$, where $d = \int(\partial_y A_+)^2 dy$. However, as pointed out by Pomeau [10], static fronts between a homogeneous and spatial periodic state may actually persist in a finite neighborhood of the Maxwell point, the *pinning range*, and it was conjectured that this phenomena could be due to nonadiabatic effects produced by nonresonant terms. This was shown in a particular case in [11] and has recently been discussed in a general frame in [12], with the conclusion that the locking phenomena results from the interaction (contained in the nonresonant terms) of the large scale envelope $A(y, \tau)$ with the small scale underlying the spatial periodic solution [11].

To describe the dynamics exhibited by (1) and the locking phenomena, we must then consider the nonresonant terms in the envelope equation (3). We consider all these terms as perturbations because they have rapidly varying oscillations. Close to the Maxwell point, we use the ansatz

$$A(y, \tau) = (A_+(y - y_0(\tau)) + \delta\rho)e^{i\delta\Theta}$$

where δ is a small parameter of order $(\epsilon - \epsilon_M)$. Introducing the above ansatz in Eq. (3) and linearizing in $\{\rho, \Theta\}$ we obtain the following solvability condition for the front's core

$$\dot{y}_0 = -\frac{\partial U(y_0)}{\partial y_0} + \frac{ab}{|\epsilon|^2}\sqrt{\frac{\eta}{2d}}\zeta(\tau) \\ = \Delta + \Gamma\cos\Big(\frac{2q}{d\sqrt{|\epsilon|}}y_0 - \varphi\Big) + \frac{ab}{|\epsilon|^2}\sqrt{\frac{\eta}{2d}}\zeta(\tau), \quad (4)$$

where $\Gamma \equiv \sqrt{k_1 + k_2} e^{-\sqrt{4/3}\pi q/d\sqrt{|\epsilon|}}$, $\tan\varphi = k_1/k_2$, $k_1 \equiv -9d\pi/2048(8q/a\sqrt{3|\epsilon|})^3 - (8 + d\pi/32\nu)(8q/a\sqrt{3|\epsilon|}) + \sqrt{3}d^2\beta^2 q^3 \eta\pi/2^3 a^3 |\epsilon|^{11/2}$, and $k_2 \equiv (27/1024 - 1/128\nu)d\pi(8q/a\sqrt{3|\epsilon|})^2 - 3d^2\beta^2 q^2 \eta\pi/2^6 a^2 |\epsilon|^5$. $U(y_0)$ is the potential which characterizes the dynamics of the front's core and $\zeta(\tau)$ is a Gaussian white noise, that is, with zero mean value and correlation $\langle \zeta(\tau)\zeta(\tau')\rangle = \delta(\tau - \tau')$.

The locking phenomena and the pinning range are simple to understand from Eq. (4); the locking phenomena is exhibited when the deterministic evolution of y_0 has stable equilibrium points, that is, the front's core has stable equilibrium positions (cf., Fig. 2). The pinning range is the parameter region where the system has equilibrium points. If $\Delta < 0$ and $|\Delta| > |\Gamma|$, the model (4) does not have equilibrium points. The front's core moves forward and its acceleration increases and decreases periodically, hence the spatial periodic state invades the homogeneous one with an oscillatory velocity. In Fig. 3, the thick and the dashed curves are the average velocity with and without noise, respectively. Increasing Δ (ϵ), the system exhibits a simultaneous infinite saddle-node bifurcations for $|\Delta| = |\Delta_-| \equiv |\Gamma|$. For $\Delta > \Delta_-$ and $|\Delta| < |\Gamma|$, the system has an infinite number of stable equilibria. Each equilibrium point represents a static front with different bumps (cf., Fig. 2). Increasing further Δ, all critical points disappear simultaneously by saddle node when $\Delta > 0$ and $\Delta = \Delta_+ \equiv |\Gamma|$. For $\Delta > \Delta_+$ the front's core moves backward, hence the homogeneous state invades the spatial periodic one with an oscillatory velocity (cf., Fig. 3). Therefore, for $\Delta_- < \Delta < \Delta_+$ (pinning range) the system exhibits the locking phenomena.

We now consider the effect of noise in (4). Because of the asymmetry of the potential and the lack of a global stationary state, the system continuously converts the random fluctuations in directed motion of the front, i.e., the noise induces front propagation. This type of phenomena is well known as a Brownian motor [13]. One can easily understand the origin of this phenomena: if initially y_0 is inside the basin of attraction Ω of a fixed point, the front just fluctuates around the fixed point during a time of the order of the mean first passage time to $\partial\Omega$, the border of Ω. After this time the system makes a transition to the basin of attraction of the nearest stable fixed point separated from the first one by the lowest energy barrier. This behavior is repeated in this new basin of attraction and the final result is a directed motion of the front. Since the energy threshold for jumping to the right or to the left is different, the probability of jumping to the side with the highest energy threshold will be exponentially small with respect to the probability of jumping to the other side and this determines the direction of motion of the front. Hence, fluctuations are privilege to the creation or removal of a bump, simply because nucleating or destroying a bump is different.

From the above analysis, we can estimate the mean velocity of the front's core

$$\langle v \rangle = \frac{\pi\sqrt{|\epsilon|}}{qa}\left(\frac{1}{\tau_+} - \frac{1}{\tau_-}\right),$$

where $\pi\sqrt{|\epsilon|}/qa$ is the distance between the two successive fixed points and $\{\tau_-, \tau_+\}$ are the escape times to move to the basins of attraction of the left or right fixed point, respectively. They have the expression

$$\left(\frac{1}{\tau_+} - \frac{1}{\tau_-}\right)^{-1} = \frac{2}{\theta}\int_{c'}^{b'}\int_{c'}^{y} e^{2(U[y]-U[z])/\theta} dy dz - \frac{2}{\theta}\int_{c'}^{a'}\int_{c'}^{y} e^{2(U[y]-U[z])/\theta} \times dy dz\left[\frac{\int_{c'}^{a'} e^{2U[y]/\theta} dy}{\int_{c'}^{b'} e^{2U[y]/\theta} dy}\right] \qquad (5)$$

where a', b', and c' are a minimum and two successive maximums of the potential $U(y_0)$ (see Fig. 2), respectively, and $\theta \equiv ab/|\epsilon|^2\sqrt{\eta/2d}$. In the limit of weak noise

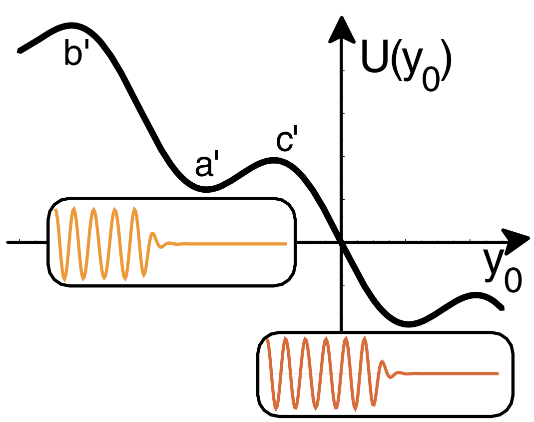

FIG. 2 (color online). Schematic representation of the potential $U(y_0)$ of Eq. (4). $\{a', b', c'\}$ are fixed points. The inset figures represent two successive equilibria states of Eq. (1).

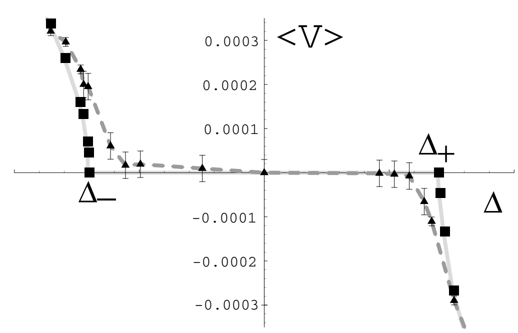

FIG. 3. Mean velocity of the front with and without noise. The thick and the dashed curves are the average velocity of the front of Eq. (1) for $\varepsilon = -0.16$, $\nu = 1.0$, $q = 0.7$, $\eta = 0.0$, and $\eta = 0.01$, respectively.

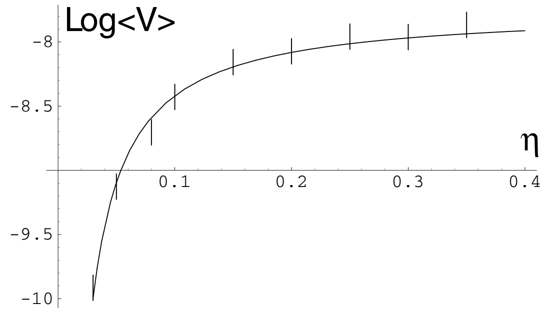

FIG. 4. Mean velocity of the front. The continuous line is the analytical formula of mean velocity and the solid dots are the numerical measuring of the mean velocity of the front of Eq. (1).

$$\langle v \rangle = \frac{2\sqrt{|\epsilon|}}{qa\sqrt{\partial_{yy}U(a')|\partial_{yy}U(c')|}} e^{-[U(c')-U(a')]/\theta} \times \left(1 - \sqrt{\frac{|\partial_{yy}U(c')|}{|\partial_{yy}U(b')|}} e^{-[U(b')-U(c')]/\theta}\right).$$

From the above expression one can find that in this limit the velocity is proportional to Kramer's rate. Numerically, we have measured the front velocity for different values of the noise intensity and we obtain a good agreement with the theoretical prediction, as it is shown in Fig. 4. It is important to remark that $U(y_0)$ is function of the noise intensity (η). For finite noise intensity this dependence is dominant in the terms k_1 and k_2, in the limit of $\epsilon \to 0$. Hence for finite noise intensity one only needs to consider the terms coming from the noise to explain the locking phenomena and the induced front propagation.

To understand the mechanism of noise-induced front propagation we have considered the subcritical Swift-Hohenberg equation. This model allows us to obtain analytical expressions for the mean velocity of the front. For an arbitrary model it is thorny to obtain explicit formulas for the front velocity, since in general we do not have access to explicit expressions of spatial periodic solutions and front solutions. Given a system that exhibits locking phenomena, close to a spatial bifurcation, one expects to find a similar envelope equation to (3) [12]. We can conclude then that the noise induces front propagation since the noise prefers to create or remove a bump, simply because the necessary perturbations to nucleate or destroy a bump are different.

The existence, stability properties, and bifurcation diagrams of localized patterns in the pinning range in one dimensional extended systems have recently been studied [14]. In one spatial dimension, one can understand the localized pattern as the equilibrium points of the front interaction [15]. When we consider the effects of noise on these solutions, we expect, due to our previous discussion, propagation of the interface of these localized patterns. From the above results, one realizes that the localized patterns are unstable in nature, that is, in the presence of noise. The velocity of propagation of the interfaces and fronts are proportional to Kramer's rate. Therefore, experimentally, one can observe these localized patterns, when noise is weak enough, for long intervals of time, as metastable states.

The simulation software DIMX developed by P. Coullet and collaborators at the laboratory INLN in France has been used for all the numerical simulations. M. G. C. and E. T. acknowledge the support of FONDECYT Projects 1051117 and 1020374, FONDAP Grant No. 11980002, and ECOS-CONICYT collaboration programs.

[1] W. Horsthemke and R. Lefever, *Noise-Induced Transition* (Springer-Verlag, Berlin, 1984).
[2] L. Gammaitoni, P. Hanggi, P. Jung, and F. Marchesoni, Rev. Mod. Phys. **70**, 223 (1998).
[3] C. Van den Broeck, J. M. R. Parrondo, and R. Toral, Phys. Rev. Lett. **73**, 3395 (1994); C. Van den Broeck *et al.*, Phys. Rev. E **55**, 4084 (1997); R. Muller *et al.*, Phys. Rev. E **56**, 2658 (1997); J. Garcia-Ojalvo *et al.*, Phys. Rev. E **54**, 6918 (1996); A. A. Zaikin, J. García-Ojalvo, and L. Schimansky-Geier, Phys. Rev. E **60**, R6275 (1999); M. Ibañes *et al.*, Phys. Rev. Lett. **87**, 020601 (2001).
[4] J. Garcia-Ojalvo, A. Hernandez-Machado, and J. M. Sancho, Phys. Rev. Lett. **71**, 1542 (1993); A. Becker and L. Kramer, Phys. Rev. Lett. **73**, 955 (1994); A. A. Zaikin and L. Schimansky-Geier, Phys. Rev. E **58**, 4355 (1998); J. Buceta *et al.*, Phys. Rev. E **67**, 021113 (2003).
[5] M. G. Zimmermann, R. Toral, O. Piro, and M. San Miguel, Phys. Rev. Lett. **85**, 3612 (2000).
[6] L. Q. Zhou, X. Jia, and Q. Ouyang, Phys. Rev. Lett. **88**, 138301 (2002).
[7] R. A. Fisher, Annals of Eugenics **7**, 355 (1937); A. Kolmogorov, I. Petrovsky, and N. Piskunov, Bull. Univ. Moskou Ser. Int. Sec. A **7**, 335 (1937).
[8] M. C. Cross and P. C. Hohenberg, Rev. Mod. Phys. **65**, 851 (1993).
[9] O. T. Valls and L. M. Lust, Phys. Rev. B **44**, 4326 (1991); J. Armero *et al.*, Phys. Rev. Lett. **76**, 3045 (1996); M. Löcher, D. Cigna, and E. R. Hunt, Phys. Rev. Lett. **80**, 5212 (1998); M. A. Santos and J. M. Sancho, Phys. Rev. E **59**, 98 (1999); Phys. Rev. E **64**, 016129 (2001); A. Rocco, U. Ebert, and W. van Saarloos, Phys. Rev. E **62**, R13 (2000).
[10] Y. Pomeau, Physica D (Amsterdam) **23**, 3 (1986).
[11] D. Bensimon, B. I. Shraiman, and V. Croquette, Phys. Rev. A **38**, 5461 (1988).
[12] P. Coullet, R. Rojas, E. Tirapegui, and C. Tresser (to be published).
[13] P. Reimann and P. Hanggi, Appl. Phys. A **75**, 169 (2002).
[14] P. Coullet, C. Riera, and C. Tresser, Phys. Rev. Lett. **84**, 3069 (2000).
[15] M. G. Clerc and C. Falcon, nlin.PS/0502041 [Physica A (Amsterdam) (to be published)].